Express Polymer Letters Vol.18, No.3 (2024) 326–336
Available online at www.expresspolymlett.com
https://doi.org/10.3144/expresspolymlett.2024.23

Research article

Enhanced thermal stability and flame retardancy of PLA through intumescent flame retardant with B-modified ZSM-5 as a synergistic agent

Xiaokun Zhai[1,2], *Qin Ma*[1], *Jing Lu*[1], *Yuwei Jin*[1], *Ruiyan Zhang*[3], *Faliang Luo*[1,2*]

[1]State Key Laboratory of High-efficiency Utilization of Coal and Green Chemical Engineering, Ningxia University, 750021 Yinchuan, China
[2]School of Chemistry and Chemical Engineering, Ningxia University, 750021 Yinchuan, China
[3]Key Laboratory of Photovoltaic Materials, School of Materials and New Energy, Ningxia University, 750021 Yinchuan, China

Received 12 September 2023; accepted in revised form 7 December 2023

Abstract. In order to improve the inherent flammability of polylactic acid (PLA) and make this new biodegradable material more widely used, B-modified ZSM-5 (B/Z5) was designed as synergistic agent of intumescent flame retardant (IFR), composed of ammonium polyphosphate (APP) and pentaerythritol (PER), and introduced into PLA/IFR (PLAs) to fabricate PLAs/B/Z5 composites by melt extrusion. The flame retardancy, surface morphology, and thermal stability of the composites were investigated by TG, LOI, UL-94, CCT, and SEM. The addition of B/Z5 makes the decomposition temperature of $T_{5\%}$ as well as $T_{10\%}$ of PLAs reduction in nitrogen atmosphere and carbon layer form in advance. UL-94 test shows the composites reach V-0 rating. LOI value also steadily increases, and the maximum value is 36.0% with B actual loading of 5.26% (recoded as 14B/Z5) in B/Z5. The PHRR decreases by 75% from 417.77 kW/m^2 for pure PLA to 103.19 kW/m^2 for PLAs/14B/Z5, and THR reduces from 92.78 to 19.26 MJ/m^2, which decreases by about 80% and the char yield reaches 50%. This study provides a simple and green method for the preparation of high flame-retardant PLA, which has a broad practical application prospect.

Keywords: *ZSM-5, PLA, Intumescent flame retardant, synergistic agent*

1. Introduction

With the continuous consumption of polymer materials, the shortage of oil resources not only is further exacerbated, but also serious ecological environment pollution is inevitable, so environmentally friendly, low-carbon, and sustainable bio-based polymer has been extensively concentrated. Polylactic acid (PLA), as a new type of biodegradable material efficiently produced by fermentation from renewable resources such as corn or potatoes [1], has been widely used in home textile clothing, packaging materials, and other fields [2–4] due to its good biodegradability [5, 6], biocompatibility, gloss, transparency and heat resistance, as well as certain bacterial resistance and UV resistance. Unfortunately, some flammable characteristics including only about 18% limit oxygen index (LOI) and easy to burn in air with severe molten drop limit PLA application in specific areas of electronic products packaging and auto industry [7, 8]. Therefore, research on flame-retardant modification of PLA is imperative.

Generally, some flame retardants have been added to the polymer to obtain flame-retardant polymer materials [9]. Recently, intumescent flame retardants

*Corresponding author, e-mail: fll@nxu.edu.cn

(IFR) have been widely researched because of their low smoke production, low toxicity, and anti-drip properties [10]. IFR is composed of an acid source, carbonization agent, and blowing agent. Currently, the most widely used IFR system is a mixture of ammonium polyphosphate (APP), pentaerythritol (PER), and melamine (MEL). According to the fire tetrahedron theory, flame combustion propagation requires four elements, including heat, fuel, oxygen as well as the chain reaction. Flame retardant play one or more roles in cutting off the contact between the four elements and the polymer matrix. By forming a carbonized layer on the surface of the composite material, IFR effectively protects the underlying polymer from thermal radiation, prevents the diffusion of oxygen, and inhibits the mass transfer of combustible gas, thus delaying the degradation of the polymer and reducing the generation of smoke.

However, the carbon layer produced by only adding IFR generally is brittleness and not very dense, so it can be easily burst by internal gas pressure and heat flow, which leads to the flame retardant performance of the polymer degradation well [11]. Luckily, adding an appropriate amount of synergistic flame retardant into IFR can effectively improve the flame retardation of the polymer. Organometallic compounds [12], montmorillonite [13], and boron compounds [14–16] have been studied as a synergistic role of catalyzing to form good mechanical and high thermal stability carbon layer. ZSM-5 zeolite is widely used in heterogeneous catalysts because of its high specific surface area, clear porosity, good thermal stability, and ability to limit metal active substances [17]. Especially, it is very easy to promote char due to good acidity and has been used as a synergistic agent of IFR [18]. For instance, Bourbigot and coworkers [19, 20] demonstrated that the addition of a small amount of 4A zeolite into IFR consisting of APP and PER promotes thermal stability of the protective carbon layer formed by zeolite catalyzing being above 550 °C. In order to further improve the catalytic coking ability of ZSM-5, H-ZSM-5 with high acidity was developed to use as a synergistic agent of IFR [21]. The results showed that the higher the concentration of acid center is, the better the catalytic effect between APP and PER becomes and the more conducive to the formation of expansive precursor.

Boron compounds were used as multifunctional flame-retardant additives for a variety of polymer materials. It is found that regardless of the type of boron compounds, the maximum decomposition temperature can be reduced, and the yield of coke can be increased. Tawiah *et al*. [22] discussed the effects of microporous boron-based expandable flame retardants on the flame retardant performance of PLA. The results show the LOI value of PLA increases steadily with the increase of the amount of flame retardant to achieve a V-0 rating. The analysis of char residue shows that the B element improves the chemical structure of the carbon layer and enhances the stability of the carbon layer by changing the formation of char residue. Although zeolite and boron-containing compounds have been widely reported as synergists, few have combined them to explore their synergistic effects on IFR [23]. The advantages of using ZSM-5 catalyst to form carbon and B to improve the carbon layer performance have aroused our interest in improving the flame retardancy of PLA. Additionally, B modified ZSM-5 generally be researched to enhance catalytic ability due to the improvement of significant acidity resulting from B electron deficient property. So, here ZSM-5 was modified with different B content as a synergist to be added into the IFR system composed of APP and PER, and their effects on the flame-retardant performance of PLA were studied in detail.

2. Experimental

2.1. Materials

Polylactic acid (PLA, Ingeo™ Biopolymer 4032D) was produced by Nature Works Ltd. (USA). Ammonium polyphosphate (APP, CAS:68333-79-9) and Pentaerythritol (PER, CAS:115-77-5) were offered by Xipaike Technology Co., Ltd. (Zhengzhou, China). ZSM-5 molecular sieve (NKF-5D-25NA) was provided by Nankai University Catalyst Co., Ltd. (Tianjin, China). Boric acid ($B(OH)_3$, 10004808) was supplied by Sinopharm Chemical Reagent Co., Ltd. (Shanghai, China). All the chemicals were used as obtained without further purification.

2.2. Preparation of B modified ZSM-5 (B/Z5)

First, as shown in Figure 1, 15 g of ZSM-5 was added to 100 mL of deionized water under ultrasound. Secondly, 0.464 g of $B(OH)_3$ was added and ultrasonicated for 30 min. After centrifugation, the sample was dried overnight at 110 °C, calcined at a heating rate of 2 °C/min in a muffle furnace from 25 to 550 °C, and kept at 550 °C for 4 h to obtain 3B/Z5 sample (3B/Z5 means that the $B(OH)_3$ used to modify

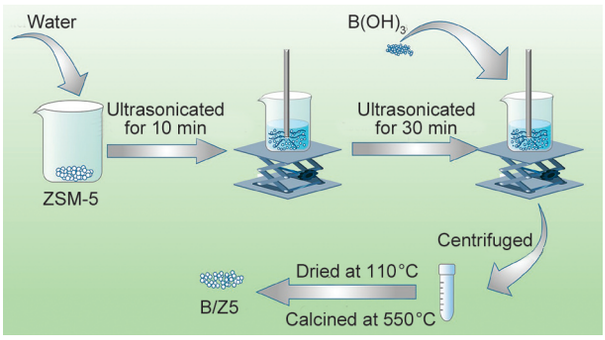

Figure 1. Schematic diagram of the preparation process of B/Z5.

ZSM-5 is only 3% of the mass of ZSM-5). A series of 7B/Z5, 10B/Z5, and 14B/Z5 samples could be obtained as the same as the preparation of 3B/Z5 by changing the addition amount of $B(OH)_3$ to 1.129, 1.67, and 2.44 g, respectively.

2.3. Fabrication of PLA and PLA composites

Firstly, PLA, APP, PER, ZSM-5 (Z5), and a series of B/Z5 samples were dried under the vacuum at 80 °C for 12 h. PLA and PLA composites were fabricated via a twin-screw extruder (SJZS-10A, Wuhan Ruiming Experimental Instrument Manufacturing Co., Ltd., China) in the temperature range from 185 to 190 °C at the screw speed of 30 rpm. Finally, the required model is moulded by injection molding machine (SZS-15, Wuhan Ruiming Experimental Instrument Manufacturing Co., Ltd., China). The formula composition and labeling of PLA and PLA composites are shown in Table 1.

2.4. Characterizations

Fourier transform infrared spectra (FTIR) (Spectrum Two, Perkin Elmer Instruments Co., Ltd., USA) were performed within the wavenumber range of 4000–400 cm^{-1} by the attenuated total reflectance (ATR) technique at room temperature.

X-ray photoelectron spectrometer (XPS) (AXIS SUPRA+, Shimadzu Corporation Co., Ltd., Japan) was used to perform elemental analysis of B/Z5.

The fire behavior for all samples was evaluated by limiting oxygen index (LOI), vertical burning (UL-94), and cone calorimeter test (CCT). The LOI was tested on a Digital Oxygen Index Tester (5801A, Suzhou Yangyi Vouch Testing Technology Co., Ltd., China) with dimensions of 130×6.5×3 mm according to ASTM D2863-97. The UL-94 test was performed on a Horizontal-vertical Burning Tester (5402, Suzhou Yangyi Vouch Testing Technology Co., Ltd., China) with a dimension of 130×13×3 mm according to ASTM D3801. The CCT was carried out on a cone calorimeter (6810, Suzhou Yangyi Vouch Testing Technology Co., Ltd., China) with dimensions of 100×100×3 mm according to ISO 5660 with a heat flux of 35 kW/m^2.

X-ray diffraction (XRD) was carried out using a powder diffractometer (D8 ADVANCEA25, Bruker AXS Co., Ltd., Germany) at Cu K_α radiation with the wavelength of 1.54 Å (λ = 1.54 Å) at room temperature. All the samples were dried in a vacuum at 130 °C for two hours before the XRD test to remove moisture.

In order to observe the morphology of char residue after CCT, Scanning Electron Microscopy (SEM) (ZEISS EVO18, Carl Zeiss AG Co., Ltd., Germany) was used at 15.00 kV.

To investigate the thermal stability of samples, thermogravimetric analysis (TGA) was performed on TA Instrument (Pyris 1, Perkin Elmer Instruments Co., Ltd., USA), all of the specimens were heated from 25 to 790 °C at a heating rate of 10 °C/min under N_2 atmosphere with a flow rate of 50 mL/min.

Table 1. The composition of PLA and PLA composites.

Sample	Composition [wt%]							
	PLA	APP	PER	ZSM-5	3B/Z5	7B/Z5	10B/Z5	14B/Z5
PLA	100	0	0	0	0	0	0	0
PLAs	85	11.25	3.75	0	0	0	0	0
PLAs/Z5	85	10.50	3.50	1	0	0	0	0
PLAs/3B/Z5	85	10.50	3.50	0	1	0	0	0
PLAs/7B/Z5	85	10.50	3.50	0	0	1	0	0
PLAs/10B/Z5	85	10.50	3.50	0	0	0	1	0
PLAs/14B/Z5	85	10.50	3.50	0	0	0	0	1

3. Results and discussions

3.1. Characterization of B/Z5 samples

To verify whether B was successfully loaded onto ZSM-5, XPS profiles of different contents of B/Z5 were characterized. Figure 2a shows the full spectrum of XPS of B-modified ZSM-5. As can be seen from Figure 2a, B1s peak (labeled by a red rectangular box in the figure) appears at 193.8 eV [24, 25], and peak height increases with the increase of B content. However, the B1s peak is not very easy to observe due to low loading, so the fine spectrum of B1s was further analyzed and shown in Figure 2b. The corresponding binding energies of 3B/Z5, 7B/Z5, 10B/Z5, and 14B/Z5 are 193.7, 193.4, 193.5 and 193.4 eV, respectively. As we all know, the peak of pure B_2O_3 is located at 193.8 eV, while the peak of $B(OH)_3$ is located at 193.4 eV [24]. So, the subtle differences in peak positions for different B/Z5 may have resulted from an increase of $B(OH)_3$ content in B/Z5 with increasing B loading on ZSM-5, implying that boric acid is not completely transformed into B_2O_3 in the calcination process under high B loading.

As can be also seen from Figure 2b, with the increase of B loading, the peak intensity in the fine spectrum increases and the peak becomes sharper. Quantitative analysis of B by XPS shows that the actual load corresponding to 3B/Z5, 7B/Z5, 10B/Z5, and 14B/Z5 were 2.57, 3.88, 4.17, and 5.26%, respectively.

Figure 2c shows the FTIR spectra of ZSM-5 and B/Z5. Two new infrared peaks at 1390 and 673 cm^{-1} can be detected and gradually increase with the increase of B content. The strong absorption peak at 1390 cm^{-1} belongs to B_2O_3, and the weak absorption peak at 673 cm^{-1} is attributed to the bending vibration of B–O–B in the borate network structure [26, 27]. The characteristic peaks at 1218 and 540 cm^{-1} are caused by the vibration of the characteristic double pentacyclic structure in ZSM-5, while the absorption peak at 790 cm^{-1} is attributed to the asymmetric stretching vibration of the internal tetrahedron of $Si(Al)O_4$ [28]. According to the above XPS and FTIR results, B was successfully loaded onto ZSM-5.

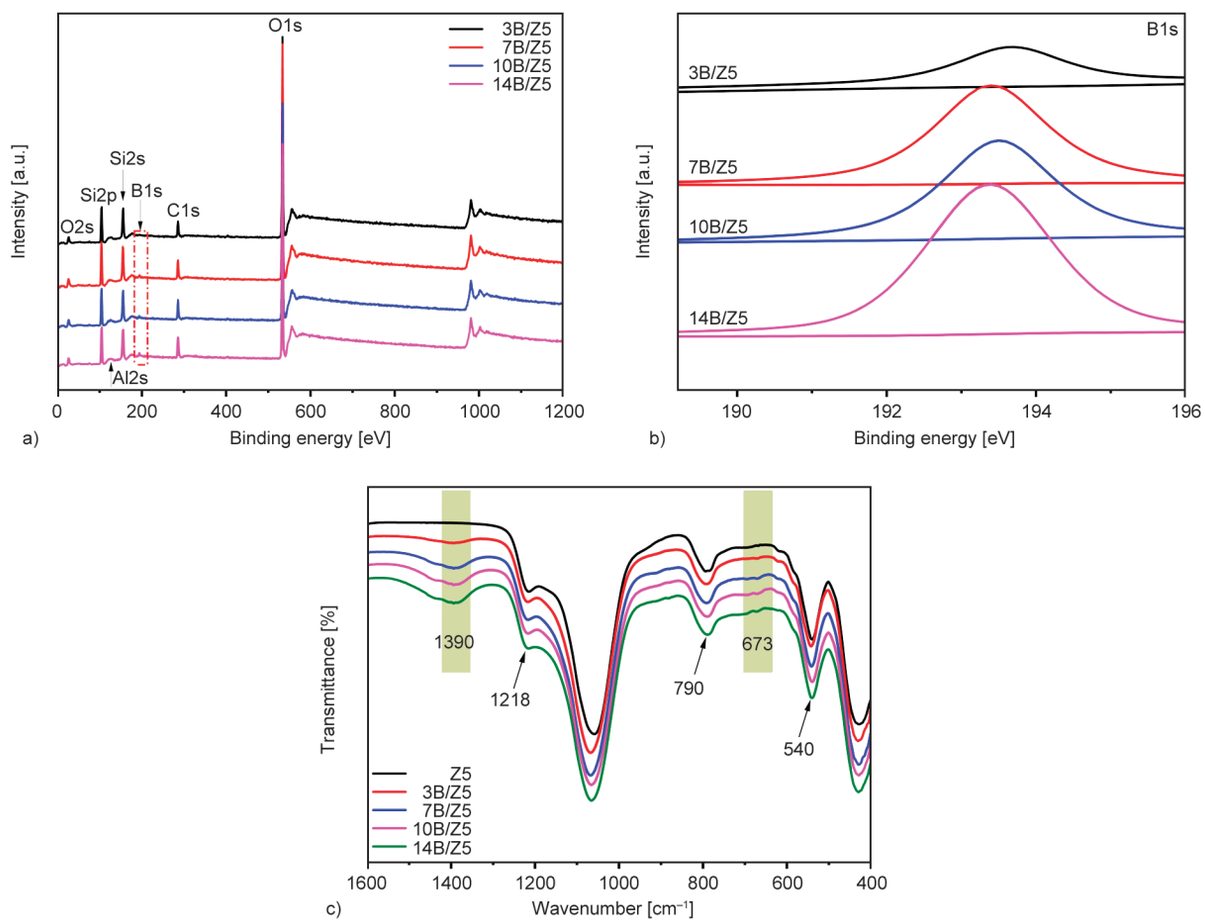

Figure 2. XPS spectra (a) and B1s spectra of 3B/Z5, 7B/Z5, 10B/Z5 and 14B/Z5 (b), FTIR spectra of ZSM-5, 3B/Z5, 7B/Z5, 10B/Z5 and 14B/Z5 (c).

3.2. Thermal degradation behavior of PLA and PLA composites

The thermal stability of PLA and PLA composites was tested by thermogravimetric analysis under a nitrogen atmosphere. TG (Figure 3a) and DTG (Figure 3b) curves are shown in Figure 3, and the corresponding specific data are listed in Table 3. Figure 3a shows all curves have a similar trend and PLA and PLA composites underwent only one step of degradation. As can be seen from Table 2, $T_{5\%}$ (the initial degradation temperature at 5% weight loss) and $T_{10\%}$ (the initial degradation temperature at 10% weight loss) of composites containing different contents and different kinds of flame-retardant additives are lower than those of pure PLA, and $T_{5\%}$ as well as $T_{10\%}$ are reduced by 24.6–69.5 and 18.1–25.2 °C, respectively. Additionally, their initial decomposition temperature is in advance. These phenomena are attributed to the decomposition of APP and the formation of a semi-coke layer by esterification and cross-linking between APP and PER, which will reduce the decomposition of the internal matrix. The corresponding temperatures of $T_{5\%}$ and $T_{10\%}$ of PLAs/Z5 are higher than composites added with B/Z5. This is because B/Z5 has a higher concentration of acidic sites and better catalytic performance, which makes the decomposition temperature of APP lower [29]. As shown in the DTG curve, compared with pure PLA, the T_{max} (the temperature at maximum decomposition rate) of all composites is shifted to a lower temperature (seen in Table 2). The char yield at 700 °C was increased to 8.60% for PLAs/14B/Z5 composites, indicating that B/Z5 and IFR have excellent synergistic effects in enhancing the charring ability of PLA.

3.3. Flame retardancy of PLA and PLA composites

Firstly, LOI and UL-94 test were used to study the flame retardation of PLA and PLA composites. Detailed data is shown in Figure 4 and Table 3. The LOI of pure PLA is 18.0%, which is ungraded based on the UL-94 test and accompanied by severe melt-dripping. The LOI of composite with the addition of IFR is 29.0% and achieves a V-0 rating based on the UL-94 test. The LOI value of the material increased slightly to 29.8% after the addition of ZSM-5, while the LOI value of the material increased from 32.7% of 3B/Z5 to 36.0% of 14B/Z5 after the addition of ZSM-5 loaded B, indicating that there is a good synergistic

Table 2. The data of PLA and PLA composites after the TG test under a nitrogen atmosphere.

Sample	$T_{5\%}$ [°C]	$T_{10\%}$ [°C]	T_{max} [°C]	Char yield at 700 °C (wt%)
PLA	337.2	346.6	366.1	–
PLAs	309.5	326.2	355.8	5.1
PLAs/Z5	312.6	328.5	354.1	7.0
PLAs/3B/Z5	293.8	324.3	358.4	6.6
PLAs/7B/Z5	310.5	327.3	354.8	6.8
PLAs/10B/Z5	267.7	321.4	356.9	6.0
PLAs/14B/Z5	291.3	323.7	357.0	8.6

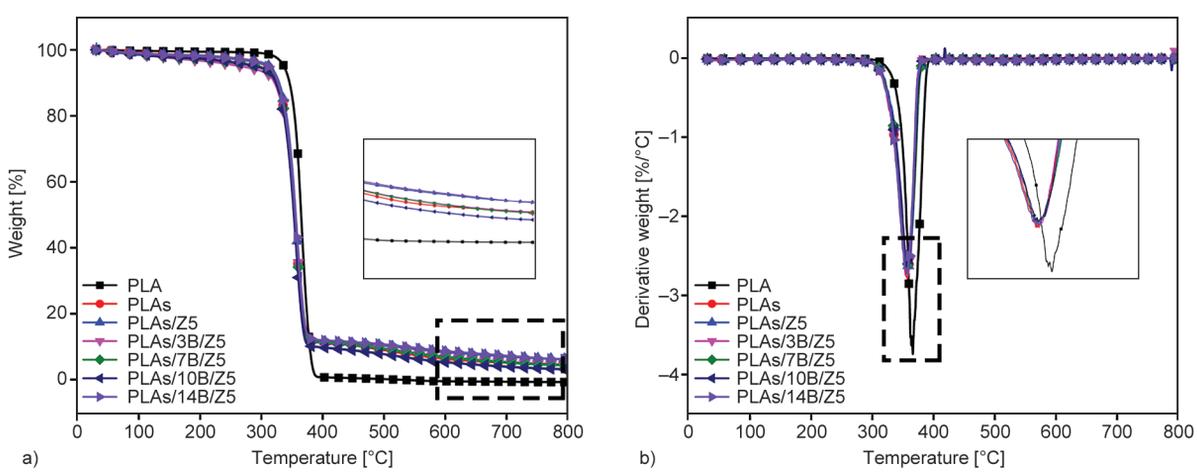

Figure 3. TG (a), DTG (b) curves of PLA and PLA composites under nitrogen atmosphere.

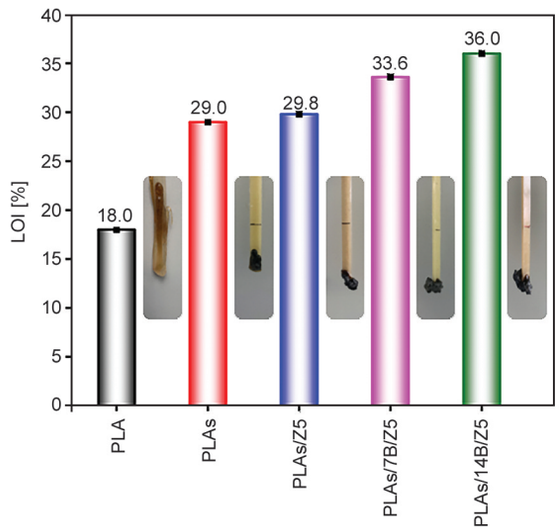

Figure 4. LOI value and digital images of PLA, PLAs, PLAs/Z5, PLAs/7B/Z5 and PLAs/14B/Z5 after LOI test.

effect between B/Z5 and IFR. Besides, all PLA composites can reach a V-0 rating in light of the UL-94 test, and the melt-dripping phenomenon is significantly improved, indicating that the addition of B can effectively inhibit melt-dripping [15, 30]. Additionally, the morphologies of various strips after LOI testing are also shown in Figure 4. It is obvious that the pure PLA appears as distinct molten droplets and no char form during the ignition process, while the char is obvious after the addition of IFR, and the amount of char gradually increases with the addition of ZSM-5 and different contents of B/Z5, displaying that the introduction of B into ZSM-5 can improve prominently the LOI value and anti-dripping ability. LOI value serves as a semi-qualitative indicator of flame-retardant effectiveness because of the requirement of small samples and low heat input. Therefore, the true fire performance of a material cannot be assessed on the basis of LOI value alone. Fortunately, cone calorimetry can simulate a real fire to analyze the burning behavior of materials from multiple angles, so it is a good reflection of the real burning situation of materials. Here, PLA, PLAs, PLAs/Z5 PLAs/7B/Z5, and PLAs/14B/Z5 were selected to be analyzed by CCT. Their heat release rate (*HRR*), mass loss (Mass), total heat release (*THR*), and total smoke rate (*TSR*) are shown in Figure 5. HRR is commonly used to assess fire intensity and spread rate. Low *HRR* values mean effective flame-retardant performance. The peak value of the *HRR* curve (*PHRR*) represents the maximum heat release ability of the material in the whole combustion process. As can be seen from Figure 5a, the *PHRR* of pure PLA is 417.77 kW/m^2, and the *PHRR* of the material decreases to 225.23 kW/m^2 after the addition of ZSM-5. The *PHRR* ulteriorly reduces to 142.08 and 103.19 kW/m^2 for PLAs/7B/Z5 and PLAs/14B/Z5 composites, respectively. Compared with pure PLA, a maximum reduction of 75% in *PHRR* can be achieved. It also can be seen that the *HRR* curve of PLA composites presents double peaks with the addition of IFR and ZSM-5 or B/Z5. The first *PHRR* is caused by the initial ignition/combustion of the surface of PLA composites under the introduction of heat flux. Once the intumescent char is formed due to the degradation of IFR, it will prevent heat and mass transfer, resulting in a sharp drop in the *PHRR*. However, the constant heat buildup causes the initial intumescent char to crack, which results in the exposure of the underlying substrate to be attacked by volatile gases and oxygen, producing the second *PHRR*. Subsequently, once enough intumescent char covering is generated again, the flame extinguishes almost immediately because the core of the flame is starved of oxygen needed for the burning to continue [11].

Flame performance index (*FPI*) and fire growth index (*FGI*) relating to *PHRR* can well characterize the potential danger of materials in fire. *FPI* is the

Table 3. LOI and UL-94 data of PLA and PLA composites.

Sample	LOI [%]	UL-94			
		AFT(s) T_1/T_2	Dripping	Cotton ignition	Rating
PLA	18.0	Burned out	Y	Y	NR
PLAs	29.0	1.0/1.1	Y	N	V-0
PLAs/Z5	29.8	1.0/0.9	Y	N	V-0
PLAs/3B/Z5	32.7	1.0/1.0	Y	N	V-0
PLAs/7B/Z5	33.6	1.2/1.3	Y	N	V-0
PLAs/10B/Z5	34.8	0.9/1.0	Y	N	V-0
PLAs/14B/Z5	36.0	1.1/1.1	Y	N	V-0

AFT: Average flaming time after the first and second ignitions.

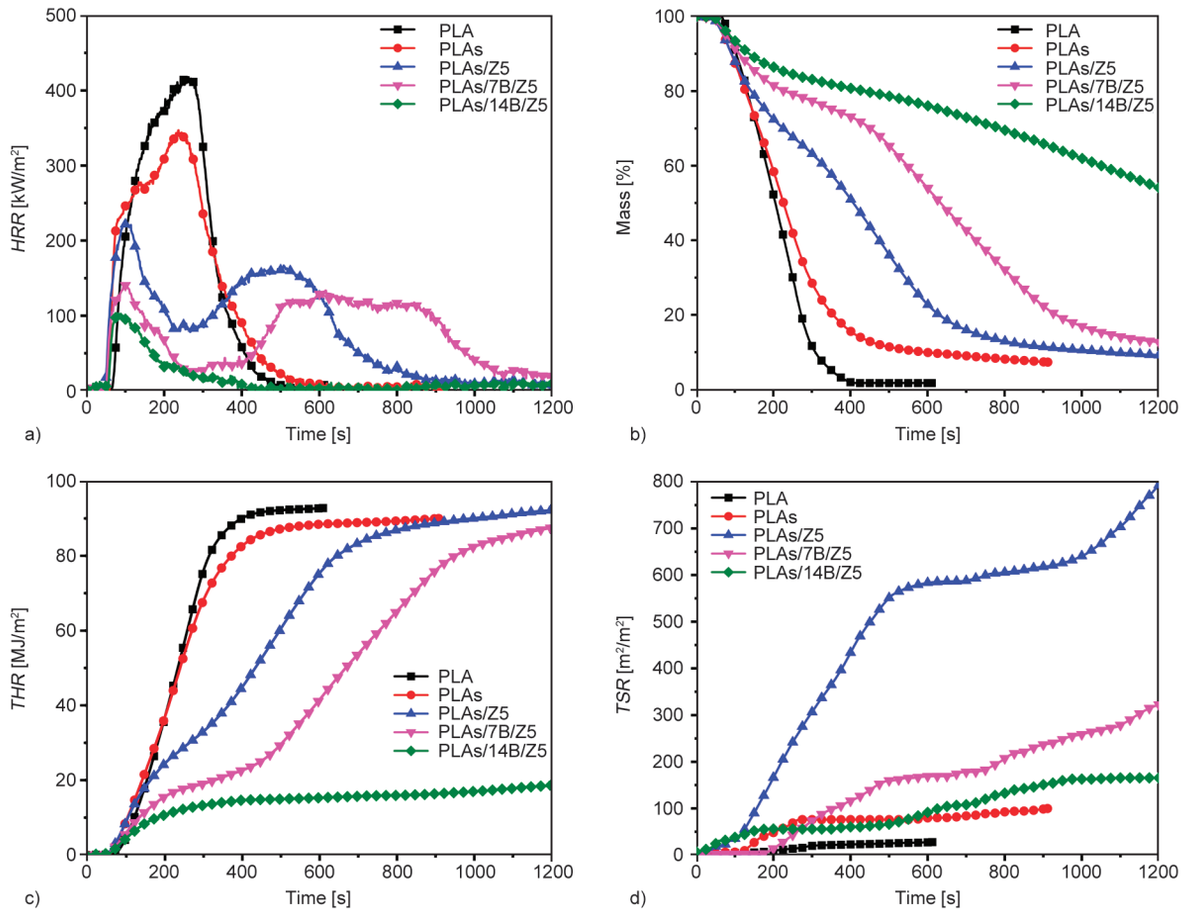

Figure 5. HRR (a), Mass loss (b), THR (c) and TSP (d) curves of PLA, PLAs, PLAs/Z5, PLAs/7B/Z5 and PLAs/14B/Z5.

ratio of the time to ignition (*TTI*) and *PHRR* value, which reflects the flaming degree. The higher the value of *FPI* is, the lower the fire risk becomes. The FGI is the ratio of *PHRR* value and time to *PHRR* (T_{PHRR}), which reflects the spread rate of fire. The smaller the *FGI* is, the longer it takes to reach a high heat release rate peak, and the smaller the fire risk gets. It can be seen from Table 4 that PLAs/14B/Z5 composite has the largest *FPI* and the smallest *FGI*, so it has the best flame-retardant performance.

Figure 5c shows the relationship of the *THR* variation with time for PLA and selected PLA composites. The *THR* curve shows that the total heat release for pure PLA is 92.78 MJ/m^2, while the *THR* of PLAs, PLAs/Z5, and PLAs/7B/Z5 is basically close to that of pure PLA, but the heat release time increase obviously. The *THR* of PLAs/14B/Z5 composite is only 19.26 MJ/m^2, which decreases by about 80% of the *THR* of pure PLA. Moreover, its final residual carbon mass reaches 50% of that of pure PLA (seen in Figure 5b). These suggest that PLAs/ 14B/Z5 can form the best isolation and protective carbon layer against the substrate LA's further combustion. On the one hand, APP and PER release small molecule gases such as H_2O and NH_3 in the process of esterification and cross-linking reaction under catalysis of ZSM-5 or B/Z5 resulting from their strong acidity. These gases can dilute the concentration of combustible gas above the combustion layer and reduce the fuel source from the outside. On

Table 4. CCT data of PLA and PLA composites.

Sample	*TTI* [s]	*PHRR* [kW/m^2]	*THR* [MJ/m^2]	Char yield [%]	Av-EHC [MJ/kg]	*TSR* [m^2/m^2]	*FPI* [m^2/(s·kW)]	*FGI* [kW/(m^2·s)]	*FRI*
PLA	64	417.77	92.78	1.72	20.38	27.75	0.15	1.59	1.00
PLAs	53	347.03	89.98	7.32	22.83	99.78	0.15	1.46	1.12
PLAs/Z5	47	225.23	92.22	9.15	21.65	801.67	0.21	2.19	0.73
PLAs/7B/Z5	49	142.08	92.04	9.98	22.48	425.45	0.35	1.44	1.12
PLAs/14B/Z5	54	103.19	19.26	49.95	19.25	165.46	0.52	1.34	5.71

the other hand, the carbon layer generated by the esterification reaction blocks the exchange between internal and external heat and combustible gas. So, the heat release and combustion intensity of the material are significantly reduced in the combustion process. Recently, Vahabi *et al.* [31] reported a general dimensionless criterion of FRI (Flame Retardancy Index, seen as Equation (1)) to evaluate the flame resistance of thermoplastic materials. The FRI of PLAs/14B/Z5 composite is 5.71 times that of PLA, showing that the PLAs/14B/Z5 have good flame retardancy.

$$FRI = \frac{\left[THR \cdot \frac{PHRR}{TTI}\right]_{\text{PLA}}}{\left[THR \cdot \frac{PHRR}{TTI}\right]_{\text{PLA composites}}} \text{ [–]} \quad (1)$$

It can be seen from the *TSR* curve (Figure 5d) that the smoke production of pure PLA is very small, and its *TSR* increases with the addition of IFR and increases sharply with the addition of ZSM-5. Especially in the scope of 200–400 s, the *HRR* of the material decreases, but the *TSR* increases linearly because ZSM-5 catalyzes the decomposition of the PLA matrix to result in incomplete combustion. But for PLA composites with B/Z5 added, *TSR* reduces with increasing B loading due to the formation of a more compact carbon layer, showing excellent smoke suppression [15].

3.4. Char analysis of PLA composites

During the combustion, the morphology and structure of the char residual were significant parameters for exploring the flame-retardant mechanism in the condensed phase. Figure 6 shows the digital photo of the positive side of the PLA composites and the SEM images of the corresponding carbon layer after the CCT. Only a small amount of char residue can be found for PLAs (seen in Figure 6a$_1$). As shown in Figure 6b$_1$–6d$_1$, the char residue gradually increases with the addition of ZSM-5 and B/Z5, and the carbon residual value is shown in Table 4. The char yield of PLAs/14B/Z5 reaches 50%. Figure 6a$_2$–6d$_2$ shows that holes and cracks of the carbon layer surface gradually become less with the introduction of ZSM-5 and B/Z5. Especially, the enhancement of B loading in ZSM-5 further reduces the holes and cracks of the carbon layer surface, even making the carbon layer surface smooth. The results show that

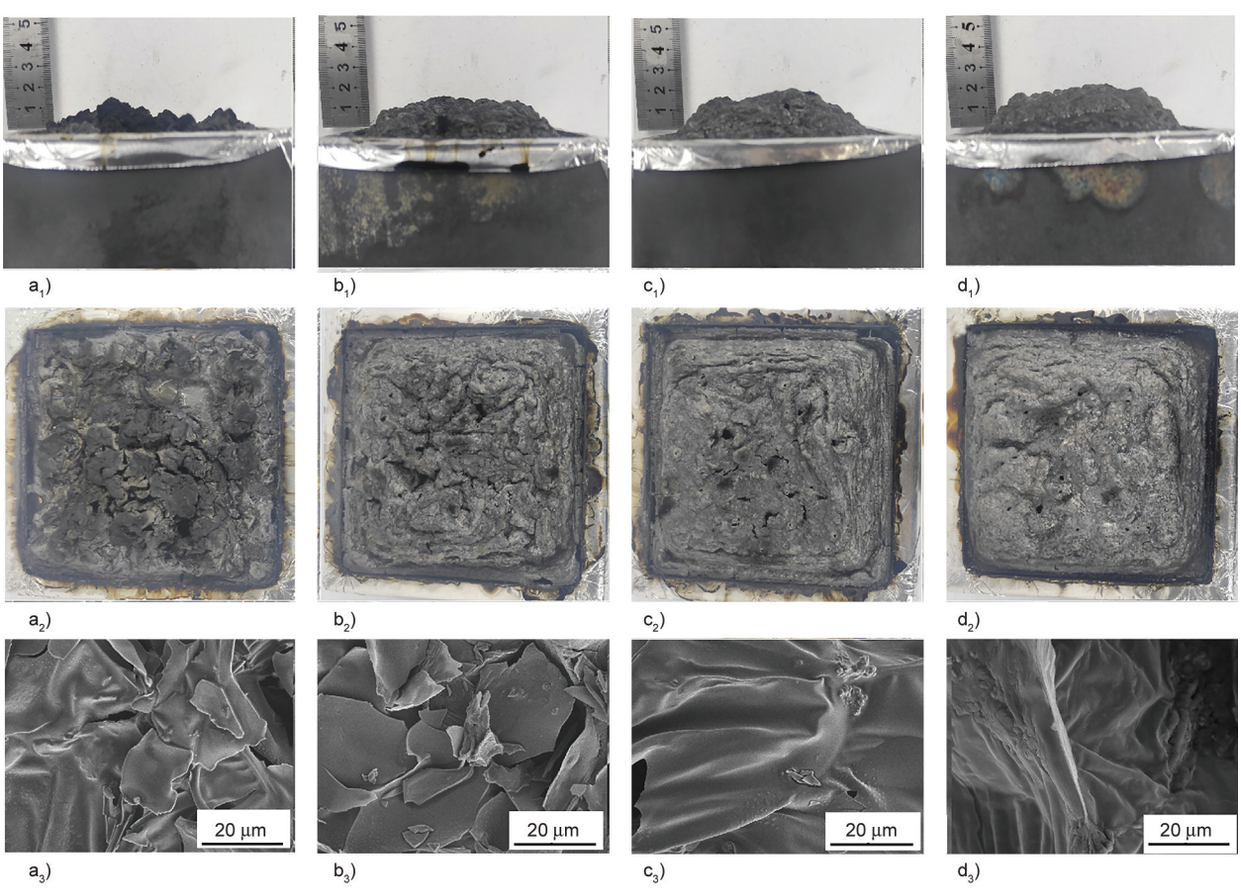

Figure 6. Side, front and SEM photographs of char residue after CCT of PLAs (a), PLAs/Z5 (b), PLAs/7B/Z5 (c) and PLAs/14B/Z5 (d), a$_1$)–d$_1$) the side photographs, a$_2$)–d$_2$) the front photographs, a$_3$)–d$_3$) SEM images of char residue.

B has the effect of stabilizing the carbon layer and making the expanded carbon layer dense and firm. Thus, a good isolation and protection effect has been achieved to result in a significant reduction in the total heat release during the whole combustion process.

SEM images of char residue after CCT are also shown in Figure 6a$_3$–6d$_3$. As seen from Figure 6a$_3$–6d$_3$, the carbon layer of PLAs displays fracture and fragments surface, indicating that the carbon layer is seriously damaged. With the addition of B/Z5, the cracking phenomenon of the carbon layer is significantly suppressed. For example, only a small amount of fracture and the surface of the carbon layer can be examined for char residue of PLAs/7B/Z5. The SEM image of char residue for PLAs/14B/Z5 composite shows that the surface is flatter and smoother, indicating that boron can improve the quality of char residue to a certain extent and ensure the compactness and integrity of the carbon layer on the surface of char residue. This means a higher flammability inhibition on materials in the later stage of combustion [9].

Figure 7 depicts the FTIR spectra of char residues of PLA, PLAs, PLAs/Z5, PLAs/7B/Z5, and PLAs/14B/Z5. For pure PLA, the absorption peaks at 1750, 1454, and 1082 cm^{-1} are assigned to the C–O and C=O. The characteristic peaks at 1607, 1132, 998, and 488 cm^{-1} are related to the C=C bond of the benzene ring structure, C–O–C, P–O–C, and O–P=O [32, 33]. The char residues with cross-linked structures can effectively slow down the heat and combustible material transfer between the gas phase and condensed phase, thus suppressing the combustion reaction of the underlying substrate. And there are characteristic peaks of B–O–C and B–O in 1452 and 1189 cm^{-1} in PLAs/7B/Z5 and PLAs/14B/Z5. This provides a continuous, dense, and toughness carbon layer structure [34].

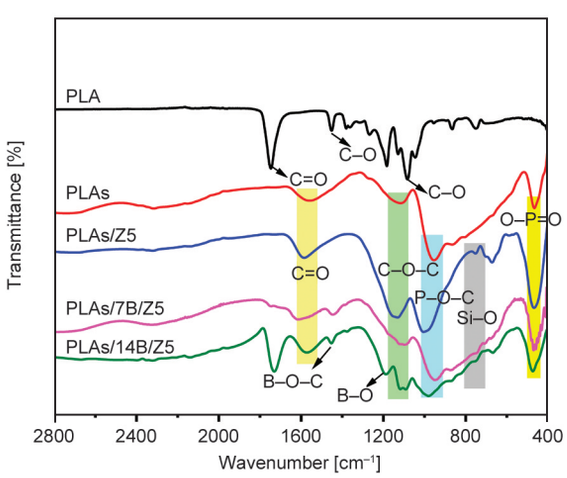

Figure 7. FTIR spectra of char residue of PLA, PLAs, PLAs/Z5, PLAs/7B/Z5, and PLAs/14B/Z5 after CCT.

4. Conclusions

In this work, the ZSM-5 molecular sieve modified B(B/Z5) is successfully prepared. And IFR with B/5 as a synergistic agent endows PLA with excellent flame retardancy. PLA composites added with 1 wt% B/Z5 and 14 wt% IFR achieve UL-94 V-0 rating while the melt-dripping phenomenon is greatly improved, and the LOI value gradually increases to 36.0% with the increase of B loading (PLAs/14B/Z5). In addition, the addition of B/Z5 makes the decomposition temperature of the material shift to low temperature under a nitrogen atmosphere, the carbon layer is preformed, and the amount of carbon slag increases significantly. The PHRR and *THR* of PLA/14B/Z5 are 75% and 80% lower than that of pure PLA, respectively. Due to the improvement of the quality of the boron-silica-containing coke layer, the heat release, smoke production in the combustion process, and cracking phenomenon of the carbon layer are all greatly improved. The combination of B/Z5 and IFR is a promising method to prepare PLA composites with outstanding flame retardancy and anti-dripping properties.

Acknowledgements

This work was supported by the Key Natural Science Foundation of Ningxia (Grant No. 2022AAC02017).

References

[1] Singhvi M. S., Zinjarde S. S., Gokhale D. V.: Polylactic acid: Synthesis and biomedical applications. Journal of Applied Microbiology, **127**, 1612–1626 (2019). https://doi.org/10.1111/jam.14290

[2] He L., Song F., Li D-F., Zhao X., Wang X-L., Wang Y-Z.: Strong and tough polylactic acid based composites enabled by simultaneous reinforcement and interfacial compatibilization of microfibrillated cellulose. ACS Sustainable Chemistry and Engineering, **8**, 1573–1582 (2020). https://doi.org/10.1021/acssuschemeng.9b06308

[3] Badia J., Gil-Castell O., Ribes-Greus A.: Long-term properties and end-of-life of polymers from renewable resources. Polymer Degradation and Stability, **137**, 35–57 (2017). https://doi.org/10.1016/j.polymdegradstab.2017.01.002

[4] Domenek S., Ducruet V.: Characteristics and applications of PLA. in 'Biodegradable and biobased polymers for environmental and biomedical applications' (eds.: Kalia S., Avérous L.), Wiley, Hoboken, 171–224 (2016). https://doi.org/10.1002/9781119117360.ch6

[5] Wen X., Liu Z., Li Z., Zhang J., Wang D-Y., Szymańska K., Chen X., Mijowska E., Tang T.: Constructing multifunctional nanofiller with reactive interface in PLA/CB-*g*-DOPO composites for simultaneously improving flame retardancy, electrical conductivity and mechanical properties. Composites Science and Technology, **188**, 107988 (2020). https://doi.org/10.1016/j.compscitech.2019.107988

[6] Jin X., Cui S., Sun S., Gu X., Li H., Sun J., Zhang S., Bourbigot S.: The preparation of an intumescent flame retardant by ion exchange and its application in polylactic acid. ACS Applied Polymer Materials, **1**, 755–764 (2019). https://doi.org/10.1021/acsapm.8b00278

[7] Olayil R., Prabu V. A., DayaPrasad S., Naresh K., Sreekanth P. R.: A review on the application of bionanocomposites for food packaging. Materials Today: Proceedings, **56**, 1302–1306 (2022). https://doi.org/10.1016/j.matpr.2021.11.315

[8] Cairns M-L., Dickson G. R., Orr J. F., Farrar D., Hawkins K., Buchanan F. J.: Electron-beam treatment of poly(lactic acid) to control degradation profiles. Polymer Degradation and Stability, **96**, 76–83 (2011). https://doi.org/10.1016/j.polymdegradstab.2010.10.016

[9] Dogan M., Dogan S. D., Savas L. A., Ozcelik G., Tayfun U.: Flame retardant effect of boron compounds in polymeric materials. Composites Part B: Engineering, **222**, 109088 (2021). https://doi.org/10.1016/j.compositesb.2021.109088

[10] Liu B-W., Zhao H-B., Wang Y-Z.: Advanced flame-retardant methods for polymeric materials. Advanced Materials, **34**, 2107905 (2022). https://doi.org/10.1002/adma.202107905

[11] Huo S., Zhou Z., Jiang J., Sai T., Ran S., Fang Z., Song P., Wang H.: Flame-retardant, transparent, mechanically-strong and tough epoxy resin enabled by high-efficiency multifunctional boron-based polyphosphonamide. Chemical Engineering Journal, **427**, 131578 (2022). https://doi.org/10.1016/j.cej.2021.131578

[12] Chen C., Song W., Jiang M., Zhang R., Li S., Cai Y., Yao J.: SiO_2/MOFs-based synergistic flame retardants provide enhanced fire safety for epoxy resins. Materials Today Communications, **35**, 105805 (2023). https://doi.org/10.1016/j.mtcomm.2023.105805

[13] Thanh T. T. N., Szolnoki B., Vadas D., Nacsa M., Marosi G., Bocz K.: Effect of clay minerals on the flame retardancy of polylactic acid/ammonium polyphosphate system. Journal of Thermal Analysis and Calorimetry, **148**, 293–304 (2023). https://doi.org/10.1007/s10973-022-11712-x

[14] Kurt R., Mengeloglu F., Meric H.: The effects of boron compounds synergists with ammonium polyphosphate on mechanical properties and burning rates of wood-HDPE polymer composites. European Journal of Wood and Wood Products, **70**, 177–182 (2011). https://doi.org/10.1007/s00107-011-0534-2

[15] Doğan M., Bayramlı E.: Synergistic effect of boron containing substances on flame retardancy and thermal stability of clay containing intumescent polypropylene nanoclay composites. Polymers for Advanced Technologies, **22**, 1628–1632 (2011). https://doi.org/10.1002/pat.1650

[16] Doğan M., Yılmaz A., Bayramlı E.: Synergistic effect of boron containing substances on flame retardancy and thermal stability of intumescent polypropylene composites. Polymer Degradation and Stability, **95**, 2584–2588 (2010). https://doi.org/10.1016/j.polymdegradstab.2010.07.033

[17] Shirazi L., Jamshidi E., Ghasemi M.: The effect of Si/Al ratio of ZSM-5 zeolite on its morphology, acidity and crystal size. Crystal Research and Technology: Journal of Experimental and Industrial Crystallography, **43**, 1300–1306 (2008). https://doi.org/10.1002/crat.200800149

[18] Ma Q., Lu J., Yao J., Yin J., Zhang R., Luo F.: The synergistic role of acidic molecular sieve on flame retardant performance in PLA/MF@APP composite. Journal of Polymer Research, **29**, 192 (2022). https://doi.org/10.1007/s10965-022-03037-y

[19] Bourbigot S., le Bras M., Delobel R., Decressain R., Amoureux J-P.: Synergistic effect of zeolite in an intumescence process: Study of the carbonaceous structures using solid-state NMR. Journal of the Chemical Society, Faraday Transactions, **92**, 149–158 (1996). https://doi.org/10.1039/FT9969200149

[20] Bourbigot S., le Bras M., Delobel R., Trémillon J-M.: Synergistic effect of zeolite in an intumescence process. Study of the interactions between the polymer and the additives. Journal of the Chemical Society, Faraday Transactions, **92**, 3435–3444 (1996). https://doi.org/10.1039/FT9969203435

[21] Bernardes F. R., Rezende M. J. C., de Oliveira Rodrigues V., Nascimento R. S. V., da Silva Ribeiro S. P.: Synthesis and application of H-ZSM-5 zeolites with different levels of acidity as synergistic agents in flame retardant polymeric materials. Polymers-Basel, **11**, 2110 (2019). https://doi.org/10.3390/polym11122110

[22] Tawiah B., Zhou Y., Yuen R. K. K., Sun J., Fei B.: Microporous boron based intumescent macrocycle flame retardant for poly(lactic acid) with excellent UV protection. Chemical Engineering Journal, **402**, 126209 (2020). https://doi.org/10.1016/j.cej.2020.126209

[23] Demirhan Y., Yurtseven R., Usta N.: The effect of boric acid on flame retardancy of intumescent flame retardant polypropylene composites including nanoclay. Journal of Thermoplastic Composite Materials, **36**, 1187–1214 (2023). https://doi.org/10.1177/08927057211052327

[24] Li H., Li H., Dai W-L., Wang W., Fang Z., Deng J-F.: XPS studies on surface electronic characteristics of Ni–B and Ni–P amorphous alloy and its correlation to their catalytic properties. Applied Surface Science, **152**, 25–34 (1999). https://doi.org/10.1016/S0169-4332(99)00294-9

[25] Gouin X., Grange P., Bois L., L'Haridon P., Laurent Y.: Characterization of the nitridation process of boric acid. Journal of Alloys and Compounds, **224**, 22–28 (1995). https://doi.org/10.1016/0925-8388(95)01532-9

[26] Ardelean I., Toderaş M., Paşcuţa P.: Structural study of the Fe_2O_3-B_2O_3-BaO glass system by FTIR spectroscopy. Journal of Optoelectronics and Advanced Materials, **3**, 1121–1123 (2006). https://doi.org/10.1142/S0217984903006098

[27] Ardelean I., Ciorcas F., Peteanu M., Bratu I., Ioncu V.: The structural study of Fe_2O_3-TeO_2-B_2O_3-SrF_2 glasses by EPR and IR spectroscopies. Modern Physics Letters B, **14**, 653–661 (2000). https://doi.org/10.1142/S0217984900000847

[28] Zhang C., Li S., Bao S.: Sustainable synthesis of ZSM-5 zeolite from rice husk ash without addition of solvents. Waste and Biomass Valorization, **10**, 2825–2835 (2019). https://doi.org/10.1007/s12649-018-0356-0

[29] Wu C., Ji D., Dong P., Li H-L., Li G-X.: The effect of boron on HZSM-5 zeolite acidity and shape selectivity. Journal of Molecular Catalysis, **33**, 524–530 (2019). https://doi.org/10.16084/j.cnki.issn1001-3555.2019.06.004

[30] Chen S., Ai L., Zeng J., Liu P.: Synergistic flame-retardant effect of an aryl boronic acid compound and ammonium polyphosphate on epoxy resins. Chemistry Select, **4**, 9677–9682 (2019). https://doi.org/10.1002/slct.201902795

[31] Vahabi H., Kandola B. K., Saeb M. R.: Flame retardancy index for thermoplastic composites. Polymers-Basel, **11**, 407 (2019). https://doi.org/10.3390/polym11030407

[32] Bao Q., He R., Liu Y., Wang Q., Zhang C.: Functionalized halloysite nanotubes endowing epoxy resin with simultaneously enhanced flame retardancy and mechanical properties. European Polymer Journal, **184**, 13 (2023). https://doi.org/10.1016/j.eurpolymj.2022.111797

[33] Fang Q., Zhan Y., Chen X., Wu R., Zhang W., Wang Y., Wu X., He Y., Zhou J., Yuan B.: A bio-based intumescent flame retardant with biomolecules functionalized ammonium polyphosphate enables polylactic acid with excellent flame retardancy. European Polymer Journal, **177**, 111479 (2022). https://doi.org/10.1016/j.eurpolymj.2022.111479

[34] Zhang T., Liu W., Wang M., Liu P., Pan Y., Liu D.: Synthesis of a boron/nitrogen-containing compound based on triazine and boronic acid and its flame retardant effect on epoxy resin. High Performance Polymers, **29**, 513–523 (2017). https://doi.org/10.1177/0954008316650929